JOURNAL OF CATALYSIS 106, 428–439 (1987)

Characterization of Iron Oxide in Fe_2O_3/SiO_2 Catalyst

TAKASHI IDA, HIDEYASU TSUIKI, AND AKIFUMI UENO

Department of Materials Science, Toyohashi University of Technology, Toyohashi, Aichi 440, Japan

KAZUYUKI TOHJI AND YASUO UDAGAWA

Institute for Molecular Science, Okazaki, Aichi 444, Japan

AND

KUMIKO IWAI AND HIROTOSHI SANO

Department of Chemistry, Tokyo Metropolitan University, Setagaya, Tokyo 158, Japan

Received October 21, 1986; revised March 10, 1987

Silica-supported iron oxide catalyst was prepared by hydrolysis of a mixed solution of ethyl silicate and iron(III) nitrate dissolved in ethylene glycol. A gel obtained by the hydrolysis was dried and calcined at various temperatures. The iron oxide particles thus prepared were maghemite (γ-Fe_2O_3), deduced by EXAFS (extended X-ray absorption fine structure) measurements and the sample color. The maghemite particles were classified into two groups: one is small but detectable by transmission electron microscopy (TEM) and the other is too small to be detected by TEM. The former was well controlled to a consistent size, which depended on the calcination temperature, and exhibited ferrimagnetic properties. The latter showed superparamagnetic properties and was estimated to be smaller than 10 Å in particle size by magnetic and Mössbauer measurements at low temperature. For comparison, the catalyst was also prepared by a conventional impregnation method using silica powder and an aqueous solution of iron(III) nitrate. Iron oxide thus prepared was hematite (α-Fe_2O_3) and the particle sizes were broadly distributed.

INTRODUCTION

Catalyst consisting of a small metal or metal oxide particle dispersed on carriers with high surface areas has been extensively studied, aiming at improved activity and selectivity for a catalytic reaction (*1*). The activity and selectivity of a supported catalyst are well known to depend upon the methods employed for the catalyst preparation. One of the reasons lies in the sizes of the metal or metal oxide particles in the catalyst. There are at least three kinds of metal atoms exposed on the surface of the particles, registered as corner, edge, and surface plane atoms, and their fractions vary with the particle size (*2*). Catalytic reactions are considered to take place on these exposed atoms with different rates and selectivities (*3*). Another reason is that metal atoms can assume several oxidation states according to the preparation conditions. The rates and selectivities of catalytic reactions strongly depend upon the oxidation states of the metal atoms (*4*).

In iron atoms of iron oxides a few oxidation states are observed: FeO, Fe_2O_3, and Fe_3O_4. In addition, two crystallographic forms are observed in Fe_2O_3: maghemite (γ-Fe_2O_3) and hematite (α-Fe_2O_3). Iron oxides have been studied as a selective catalyst for the production of butadiene in the partial oxidation of butene. Misono *et al.* (*5*) studied the catalytic performances of unsupported α-Fe_2O_3, γ-Fe_2O_3, and Fe_3O_4 for oxidative dehydrogenation of butene and reported that γ-Fe_2O_3 exhibited the highest activity and selectivity of these

0021-9517/87 $3.00

three types of iron oxides. An attempt to disperse fine maghemite particles over a silica surface has been made by Lunde and Dumesic (*6*). They found that Fe_3O_4 was converted to γ-Fe_2O_3 but not to α-Fe_2O_3 during oxidation of the catalyst and interpreted in terms of a particular interaction of Fe_3O_4 with the silica support. This interaction was believed to be attributed to the substitution of Si^{4+} ions with Fe^{3+} ions in tetrahedral sites of Fe_3O_4 spinel at their interface. Yang *et al.* (*7*) recently reported, however, that only α-Fe_2O_3 was observed in calcined silica-supported iron oxide catalyst but no trace of γ-Fe_2O_3 was identified. In their subsequent paper (*8*) the selectivity of the Fe_3O_4 catalyst for the production of butadiene was reported to increase up to 80%, from less than 50%, with the decrease in the particle size of Fe_3O_4.

Under these circumstances it has been desirable to develop techniques to control the oxidation states and the particle sizes of iron oxides in supported catalysts. In our previous paper (*9*) it was emphasized that fine metal or metal oxide particles of a consistent size were produced when metal nitrate dissolved in ethylene glycol and ethyl silicate were employed as starting materials for silica-supported metal or metal oxide catalyst. This technique for catalyst preparation was called the alkoxide technique and was applied to the preparation of the silica-supported iron oxide catalyst in the present work. It was also emphasized in our previous paper (*10*) that EXAFS (extended X-ray absorption fine structure) spectroscopy is a useful tool with which to characterize fine particles in catalysts. Therefore, the iron oxide particles dispersed in the silica support were characterized by means of EXAFS as well as Mössbauer spectroscopy and magnetic measurements. XRD (X-ray diffractometry), TEM (transmission electron microscopy), and infrared spectroscopy were also employed to reveal the structural features of the iron oxide particles. For comparison, the iron oxide particles in the silica-supported catalyst prepared by a conventional impregnation method were also studied.

EXPERIMENTAL

1. Catalyst preparation. The catalyst employed was silica-supported iron oxide, prepared by hydrolysis of a mixed solution of ethyl silicate and iron(III) nitrate dissolved in ethylene glycol at 353 K. A gel thus prepared was dried at 383 K for 24 h, followed by calcination in air at the desired temperatures for 4 h. The iron concentration in the catalyst was 10 wt%. The catalyst thus prepared is designated catalyst A. The preparation procedures of the catalyst A are summarized in Table 1.

The catalyst called catalyst I was prepared by impregnating silica powder with an aqueous solution of iron(III) nitrate. The impregnated powder was dried at 383 K for 24 h and then calcined at 773 K for 4 h. The iron concentration in catalyst I was also 10 wt%. The silica powder employed was prepared by hydrolysis of ethyl silicate at 353 K and the surface area was 410 m^2/g by the BET method using nitrogen at its liquid temperature.

2. XRD and EXAFS measurements. The catalyst powder was subjected to XRD analysis. An X-ray diffractometer (Rigaku-Denki Co., Geigerflex) was operated at 30 kV with a filament current of 15 mA using a Ni filter for Cu$K\alpha$ radiation with a wavelength of 1.542 Å. The crystalline size of the iron oxide in catalyst I was estimated by the width at half-height using Sherrer's equation (*11*).

TABLE 1

Preparation Procedures of Silica-Supported Iron Oxide Catalyst by Alkoxide Method

1	$Fe(NO_3)_3$ dissolved in ethylene glycol at 353 K
2	Addition of $Si(OC_2H_5)_4$ at 353 K with stirring
3	Hydrolysis at 353 K with stirring for 5–10 h, a gel is formed
4	Drying at 383 K for 24 h
5	Calcined at various temperatures for 4 h in air

An in house EXAFS spectrometer employed in the present work has already been described (*12*). The experimental conditions and the methods of the data analyses were almost the same as those mentioned in a previous paper (*10*), except that Ge(311) crystal was employed as a dispersing element with a slit width of 500 μm. The resolution is about 4.5 eV, estimated from FWHM (full-width half-maximum) measurements of *W* $L\alpha$ line. In order to diminish the adsorption by air, a He path was used for the EXAFS measurements. The sample powder was diluted by an appropriate amount of boron nitrite, if necessary, and all the measurements were made at room temperature.

3. TEM measurements. The particle size of the iron oxide in the catalyst was monitored by a TEM (Hitachi, H-800), operated at an accelerating voltage of 200 kV with the magnification of 10^5. The photographs were enlarged two to four for reproduction. About 10^3 particles in the photographs were measured in each catalyst to obtain the size distribution curve.

The sample powder was first ground with an agate mortar and then suspended into ethanol with an aid of supersonicant. The fine part of the suspension liquid was pipetted over a microgrid to be subjected to TEM measurements.

4. Magnetic measurements. Since the iron oxide in catalyst A was proved to be maghemite (γ-Fe_2O_3) by EXAFS measurements, the magnetic property was measured with a vibrating sample magnetometer (Toei-Kogyo Co., VSM-2) with a vibrating frequency of 80 Hz and a magnetic field up to 2 T. Most of the measurements were carried out at room temperature. The magnetic measurements at low temperatures (4.5–290 K) were performed with a Faraday-type magnetometer at the Institute for Molecular Science. The magnetometer was equipped with a superconductive magnet (Oxford Co.), supplying a magnetic field up to 5 T, and with a cryostat available at liquid He temperature. The sample temperature was measured by a carbon or platinum resistance thermometer. The details of the apparatus have been described elsewhere (*13*).

5. Mössbauer spectroscopy. The Mössbauer spectrometer system used in the present work has been described in a previous paper (*14*). In short, it consists of a radioactive source (^{57}Co diffused into rhodium) and a proportional counter connected to a multichannel analyzer for the data collection. The signals were accumulated for 72 h and then treated with a computer system developed at Tokyo Metropolitan University. A cryostat available at liquid He temperature was used for the measurements at low temperatures. The samples were ground, mounted on aluminum foil, and then placed at a proper position in the cryostat.

6. Infrared spectroscopy. The interaction between fine maghemite particles and the silica support was studied by means of infrared spectroscopy (JASCO, IR-3A) with a conventional KBr method. The measurements were carried out at room temperature in the wavenumber range of 700 to 4000 cm^{-1}.

RESULTS AND DISCUSSION

1. XRD and EXAFS Analyses

For catalyst I the X-ray diffraction peaks assigned to α-Fe_2O_3 were clearly observed and grew with calcination temperature, as shown in Fig. 1. From these diffraction peaks the mean crystalline size of the hematite in catalyst I was roughly estimated using Sherrer's equation. The size increased with elevation of the calcination temperature (Fig. 2).

For the catalyst A, no diffraction peaks were observed even when the catalyst was calcined at 1273 K for 4 h, suggesting that the iron oxide particles in catalyst A are very small. Accordingly, an EXAFS study was carried out to identify the chemical species of iron oxide in the catalyst. In Fig. 3 are shown the Fe EXAFS spectrum of

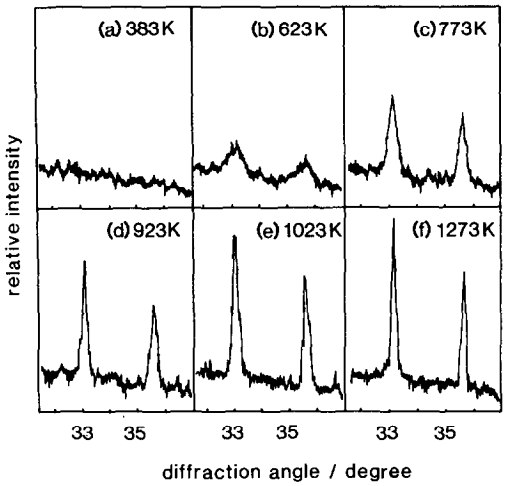

FIG. 1. X-ray diffraction patterns of catalyst I calcined at various temperatures.

catalyst A calcined at 773 K and its associated Fourier transform. For comparison, the EXAFS spectra of standard samples of α-Fe_2O_3, γ-Fe_2O_3, and Fe_3O_4 are depicted in Fig. 4 with their associated Fourier transforms. As will be mentioned below, the iron oxide in catalyst A exhibits a ferrimagnetic property, indicating that the iron oxide should be assigned as either γ-Fe_2O_3 or Fe_3O_4. Comparing the Fourier transform of catalyst A with the transforms of the standard γ-Fe_2O_3 and Fe_3O_4, the peaks due to Fe–O and Fe–Fe bondings appeared at the same positions in these three transforms, although the peak intensities are quite different. Thus, the EXAFS measurements

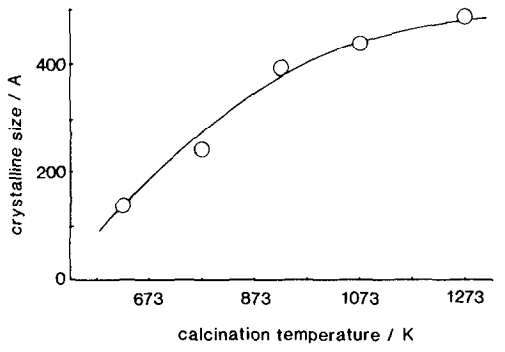

FIG. 2. Change in the particle size of α-Fe_2O_3 in catalyst I with calcination temperature.

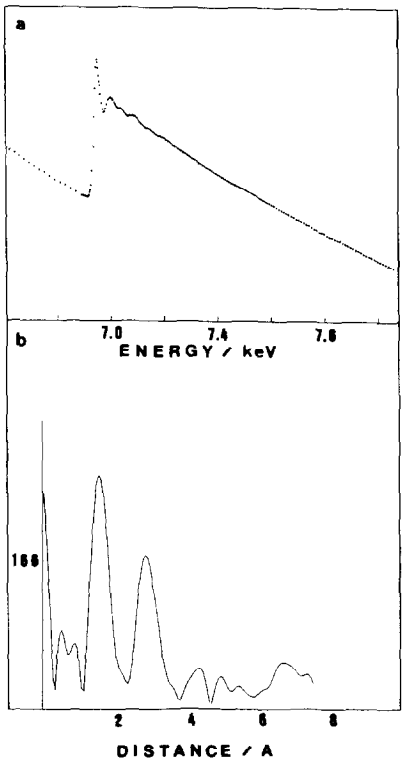

FIG. 3. EXAFS spectrum of iron oxides in catalyst A calcined at 773 K (a) and the associated Fourier transform (b).

also suggest that the iron oxide in calcined catalyst A is either γ-Fe_2O_3 or Fe_3O_4. The curve-fitting technique often employed for the determination of chemical species (*15*) is of no use in the present case, since the crystallographic structure of γ-Fe_2O_3 is a defect spinel with a lattice constant of 8.30 Å (*16*). The color, however, can be evidence that the iron oxide is γ-Fe_2O_3 and not Fe_3O_4, since Fe_3O_4 is black and γ-Fe_2O_3 is red brown. The difference in the peak intensities of their Fourier transforms indicates that the iron oxide (γ-Fe_2O_3) particles in catalyst A are very small. The peak intensities in the Fourier transform of small particles decrease with increasing distance from the central absorbing atom and the mean particle size can be roughly estimated from the transforms using the techniques developed by Greegor and Lytle (*17*) and applied by the present authors (*18*). The

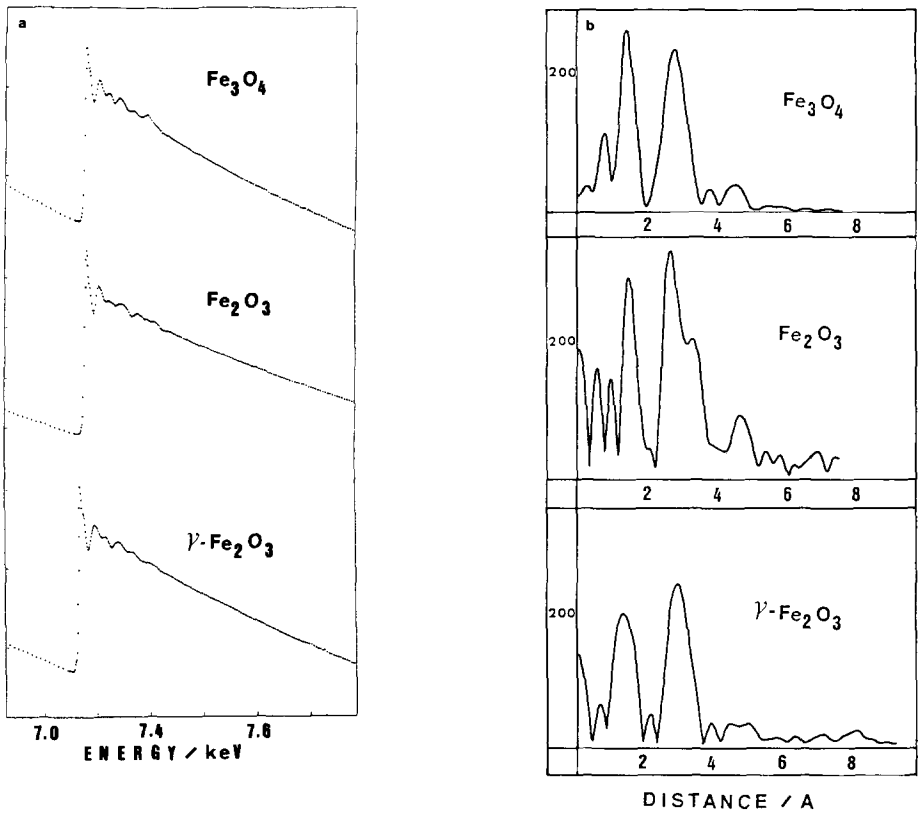

FIG. 4. EXAFS spectra of standard samples of α-Fe_2O_3, γ-Fe_2O_3, and Fe_3O_4 (a) and their associated Fourier transforms (b).

resulting value is around 10 Å, in contrast to the results obtained from TEM measurements mentioned below.

2. *TEM Measurements*

Typical photographs of the iron oxide particles in catalysts I and A calcined at 773 K are shown in Fig. 5, showing that the particles in the catalyst A are a consistent size but those in the catalyst I are not. The size distribution curves obtained from these photographs are depicted in Fig. 6. The sharp distribution curve was obtained for the iron oxide particles in catalyst A, being characteristic of the alkoxide technique for the preparation of catalysts (*19*). The mean particle size obtained by the equation $d = \Sigma_i\ n_i d_i / n_i$ for the size distribution curve varied with the calcination temperature, as shown in Fig. 7. The size of the iron oxide (γ-Fe_2O_3) particles in catalyst A increased with increasing calcination temperature and no particles were observed by TEM in dried catalyst A. The mean particle size in catalyst A calcined at 773 K is about 60 Å, inconsistent with the particle size estimated by EXAFS measurements. This might be due to the lower limit of the TEM employed in this work. The smaller the particles, the less contrast is observed in the photograph. Consequently, it is suggested that there are at least two kinds of iron oxide particles in catalyst A: one is small but detectable by TEM, the size still being well controlled at a consistent level and the level varying with the calcination temperature, and the other is too small to be observed by TEM.

3. *Magnetic Measurements at Room Temperature*

Since the iron oxide in catalyst I is proved to be hematite (α-Fe_2O_3), an antifer-

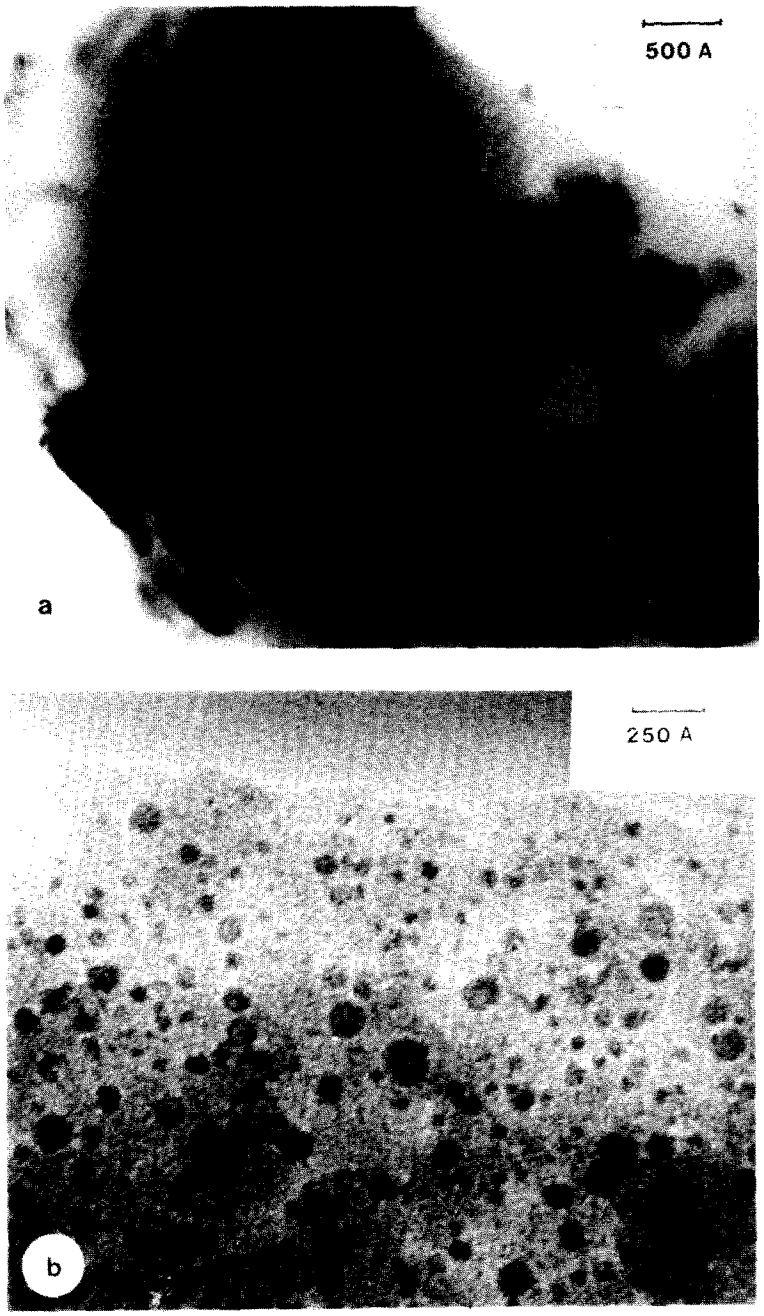

FIG. 5. Typical micrographs of iron oxide particles in catalyst I (a) and A (b) calcined at 773 K.

romagnetic substance, the magnetic measurements were performed only for the iron oxide (γ-Fe_2O_3) in catalyst A. The magnetization curves of the dried and calcined catalyst A are demonstrated in Fig. 8, where the magnetizations are expressed in terms of electromagnetic units per gram (emu/g) of catalyst powder. Besides the dried sample, the magnetizations increased rapidly for the first 0.3 T of the magnetic field and then gradually increased with the field strength up to 2 T. This seems to

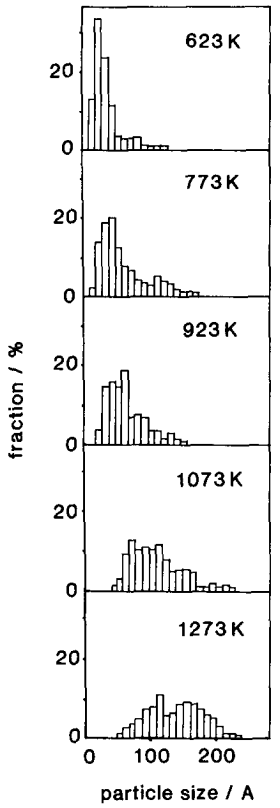

FIG. 6. Change in the particle size distribution of iron oxide in catalyst A with calcination temperature.

indicate that the iron oxide particles in calcined catalyst A are classified in at least two groups: one shows a rapid response to the applied magnetic field and the other is magnetized proportionally to the strength

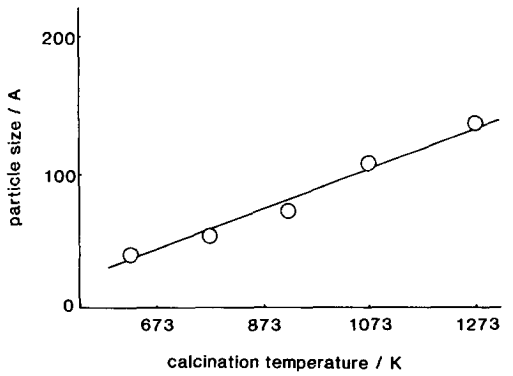

FIG. 7. Change in the mean particle size of iron oxide in catalyst A with calcination temperature.

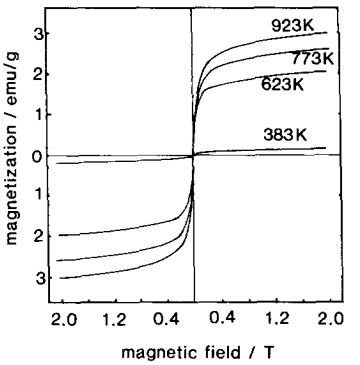

FIG. 8. Magnetization curves of catalyst A calcined at various temperatures.

of the applied field. The former is rather ferrimagnetic and might be attributed to the particles observable by TEM and the latter is superparamagnetic and might be the particles undetectable by TEM. The small coercive forces (around 20 Oe for any calcined samples) shown in Fig. 8 show that the particles observable by TEM are still fine. The iron oxide particles in dried catalyst A were hardly magnetized and their magnetizations were quite proportional to the applied magnetic field, indicating that the particles are superparamagnetic. This is very consistent with the fact that no particles were detected by TEM in dried catalyst A.

In Fig. 9 is shown the change in the magnetization of catalyst A at 2 T with the calcination temperature. The magnetization increased with increasing calcination temperature up to 923 K and then rapidly decreased. The increase in the magnetization up to 923 K is attributed the particle growth of the iron oxide (γ-Fe_2O_3) and the rapid decrease at the higher temperatures is ascribed to the conversion of γ-Fe_2O_3 to α-Fe_2O_3, since α-Fe_2O_3 is a more stable species under these conditions.

4. Magnetic Measurements at Low Temperature (4.5–290 K)

The magnetization curves of catalyst A calcined at 773 K were measured at low temperatures (Fig. 10) and the change in the

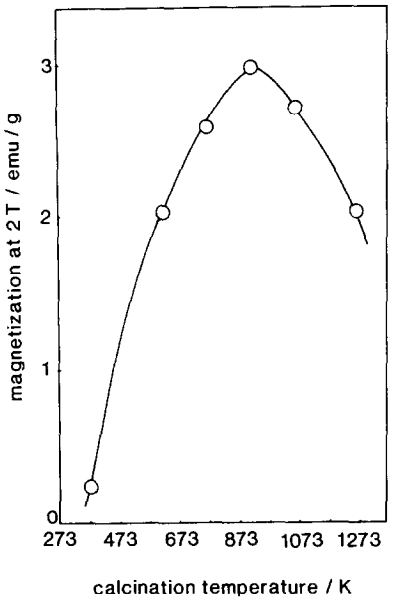

FIG. 9. Change in the magnetization of catalyst A at 2 T with calcination temperature. (Measurements were done at room temperature.)

magnetization at the magnetic field of 5 T was plotted against sample temperature (Fig. 11). The magnetization at 5 T gradually increased with decreasing the sample temperature and rapidly increased at the temperatures lower then about 50 K. This indicates again that at least two kinds of iron oxide particles are present in calcined catalyst A: One is superparamagnetic, showing a rapid increase in magnetization at the temperatures less than 50 K, probably due to the reduction in thermal movements of the particles at low temperature. The other is ferrimagnetic and all the magnetic momenta of the particles are completely oriented with the direction of the applied field. The latter is the iron oxide particles sized about 60 Å, as already measured by TEM.

By extrapolating the linear part of the curve shown in Fig. 12, the magnetization of the ferrimagnetic particles at 0 K with the field strength of 5 T was estimated, 3.65 emu/g. Similarly, the magnetization at liquid He temperature (4.5 K) was estimated to be 3.6 emu/g of catalyst powder. The expected magnetization curve of the ferrimagnetic particles in calcined catalyst A at 4.5 K is shown by the solid curve in Fig. 10 (designated 4.5 est.). The curve of 4.5 est. was drawn similarly to the curve at 290 K, since the magnetization of the superparamagnetic particles might con-

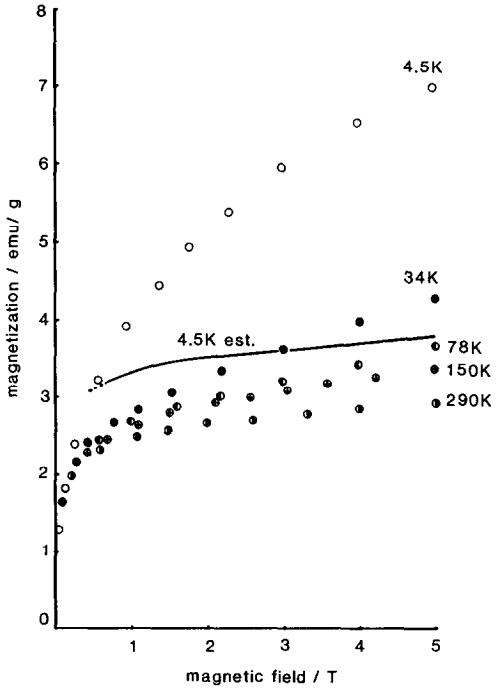

FIG. 10. Low-temperature magnetization curves of catalyst A calcined at 773 K.

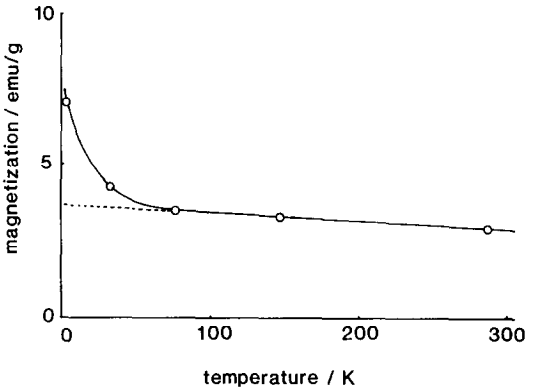

FIG. 11. Change in the magnetization of catalyst A at 5 T with temperature.

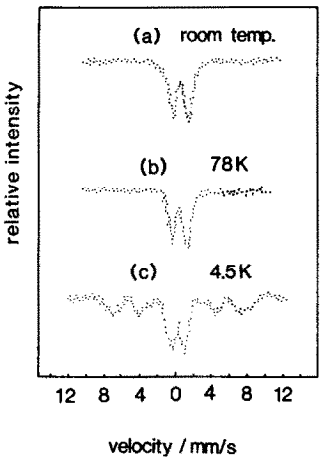

FIG. 12. Mössbauer spectra of iron oxides in catalyst A calcined at 773 K. (a) At room temperature, (b) at 78 K, and (c) at 4.5 K.

tribute less at this temperature. Accordingly, the differences between the curves designated 4.5 K and 4.5 est. are attributed to differences in the magnetizations of the superparamagnetic particles at the liquid He temperature with the corresponding magnetic fields. The magnetizations of the superparamagnetic particles in calcined catalyst A at 4.5 K are thus estimated (*20*) and are summarized in Table 2.

5. *Mössbauer Spectroscopy*

Mössbauer spectra of the iron oxide in calcined catalyst A are shown in Fig. 12. The spectrum measured at the liquid He temperature consists of two components: a central doublet and a hyperfine-split component. The central doublet is attributed to iron oxide particles behaving superparamagnetically, while the magnetically split sextuplet, which was negligibly observed at liquid N_2 temperature, is caused by the presence of the iron oxide particles exhibiting ferrimagnetic properties (*20*). This is very consistent with the results mentioned above. The isomer shift estimated from the central doublet is about 0.35 mm/s and is significantly smaller than that of bulk maghemite, 0.5 mm/s, with respect to metallic iron. This suggests that the electronic states of Fe ions in the superparamagnetic particles are quite different from those in the bulk maghemite because of the bond formation, such as Si–O–Fe, proposed as a strong oxide–oxide interaction between the superparamagnetic oxides and silica support (*6*). The magnetic split of the sextuplet, caused by the ferrimagnetic particles, is about 450 kOe and is also much smaller than that of the bulk value, about 520 kOe at liquid He temperature. The reduced split of sextuplet has been observed often (*21*) and is attributed to the collective magnetic excitations in small particles (*22*).

By computer fitting applied to the combined spectra of the central doublet and the sextuplet, the fraction of iron atoms in the

TABLE 2

Calculation of Langevin Function Using the Results Shown in Fig. 11

Magnetic field (kOe)	Magnetization (emu/g)	$c = 2 \times 10^{-5}$		$c = 4 \times 10^{-5}$		$c = 6 \times 10^{-5}$	
		$a = cH$	$L(a)$	$a = cH$	$L(a)$	$a = cH$	$L(a)$
10	0.93	0.2	0.0665	0.4	0.132	0.6	0.195
15	1.60	0.3	0.0994	0.6	0.195	0.9	0.285
20	2.13	0.4	0.131	0.8	0.256	1.2	0.366
25	2.60	0.5	0.164	1.0	0.313	1.5	0.438
30	3.07	0.6	0.195	1.2	0.366	1.8	0.500
35	3.47	0.7	0.226	1.4	0.415	2.1	0.552
40	3.73	0.8	0.255	1.6	0.460	2.4	0.599
45	4.13	0.9	0.285	1.8	0.500	2.7	0.637
50	4.27	1.0	0.313	2.0	0.537	3.0	0.672

superparamagnetic particles was calculated by measuring the percentage of the total spectral area present as a central superparamagnetic doublet. It was proved that about 75% of the iron atoms in calcined catalyst A are contained in the superparamagnetic particle fraction and the other 25% are in the ferrimagnetic particle portion. The details of the technique employed for the calculation has been mentioned elsewhere (*23*).

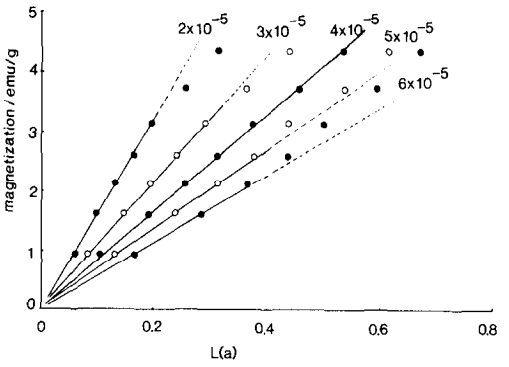

FIG. 13

6. *Estimation of the Size of Superparamagnetic Particle*

It is obvious in the results and discussion above that two kinds of maghemite particles exist in calcined catalyst A: One is ferrimagnetic and detectable by TEM, the size being controlled in an even level. The other is superparamagnetic and is too small to be detected by TEM. The size of the latter particles was roughly estimated by EXAFS to be around 10 Å. In this section the size of the superparamagnetic particles is discussed in regard to the results obtained by magnetic and Mössbauer measurements at liquid He temperature, although the time scale for superparamagnetism is different for magnetic susceptibility and Mössbauer spectroscopy. The estimation of size was carried out according to the method proposed by Okamoto *et al.* (*20*).

If the size of the particles is relatively uniform, a single Langevin function below will be satisfied with a proper variable of c. The single Langevin function is expressed as

$$M = M_s \cdot L(a), \quad a = cH \text{ and } c = \mu/kT,$$

where M and M_s are the magnetization at a certain field strength and the saturation magnetization, respectively, μ is a magnetic momentum of the particle of interest, and k is Boltzmann constant. Since the values of M are summarized in Table 2, the calculations were carried out with various c values. As seen in Fig. 13, a linear relationship between M and $L(a)$ was obtained when c was taken to be 4×10^{-5}. The results obtained are also summarized in Table 2.

The magnetic momentum of a superparamagnetic particle was calculated using $\mu = ckT$ and the value of 2.67 μ_B was obtained, while the magnetic momentum of an iron ion in the superparamagnetic particle can be estimated from the slope of the line ($c = 4 \times 10^{-5}$) in Fig. 13, and the value of 0.13 μ_B was obtained. Thus, a superparamagnetic particle is found to contain about 20 (2.67/0.13) iron atoms. The iron oxides in catalyst A are ascribed to maghemite, by EXAFS, and the maghemite is a defect spinel with 21 iron atoms in a unit cell (*16*).

These considerations led us to the conclusion that the size of the superparamagnetic particles in catalyst A is about an order of a unit cell of maghemite (γ-Fe_2O_3) dispersed in a silica network. It may be possible that the unit cells are formed during drying the gel obtained by hydrolysis, since no particles were observed by TEM in the dried sample and no ferrimagnetic properties were detected by the magnetic measurements. The iron atoms in the unit cell are believed to be bound to Si atoms in a silica network, forming Fe–O–Si bondings which were observed by the infrared spectroscopy.

7. Infrared Spectroscopy

Infrared spectra of calcined catalyst A and silica powder are shown in Fig. 14. The absorption peaks observed at 800 and 1070 cm^{-1} are assigned to the symmetric and asymmetric stretching modes of Si–O–Si structures in a SiO_2 network. The peak at 950 cm^{-1} is probably due to the presence of a Si–O–Fe structure since Si–O–M bonding, where M represents a metal atom such as Al, Ti, Zr, Ge, or Ni, has been reported to show an additional absorption peak between 800 and 1100 cm^{-1} (*24*). The presence of the Si–O–Fe structures in catalyst A is evidence of the strong oxide–oxide interaction (*6*) between the iron oxides and the silica support. No such an absorption peak was observed in the spectrum of catalyst I.

CONCLUSION

On the basis of the present results, the mechanism of the formation of maghemite particles in calcined catalyst A is concluded as follows: First, iron atoms are atomically dispersed in the gel obtained by hydrolysis of a mixed solution of ethyl silicate and iron(III) nitrate dissolved in ethylene glycol, since it has been already proved that nickel atoms are atomically dispersed in the gel prepared by similar techniques using nickel nitrate (*9*). These highly dispersed iron atoms coagulate to form small maghemite particles during drying at 383 K, the size being around 10 Å. These small particles might be unit cells of maghemite (γ-Fe_2O_3), exhibiting superparamagnetic properties. A part of the cells moved around in the SiO_2 network during the calcination and coagulate again to form ferrimagnetic particles, detectable by TEM. The fraction of iron atoms in the ferrimagnetic particles to the total iron atoms in the catalyst depends upon the calcination temperature. When the catalyst was calcined at 773 K, the fraction was estimated to be about 25 at.%.

A question still remains why the iron oxide in calcined catalyst A is maghemite (γ-Fe_2O_3) and not hematite (α-Fe_2O_3); nevertheless the hematite is known to be more stable than the maghemite under the conditions employed. The reason is not clear but it should be mentioned that when aqueous iron (III) nitrate or iron(III) isopropoxide dissolved in isopropanol was employed as the starting material, instead of iron(III) nitrate dissolved in ethylene glycol, the iron oxide in the calcined catalyst was found to be hematite, not maghemite. This seems to mean that a divalence alkoxide such as ethylene glycolate is necessary for the preparation of maghemite particles.

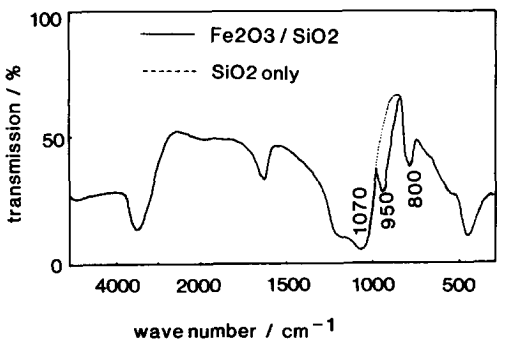

FIG. 14

ACKNOWLEDGMENTS

The present authors express their thanks to Dr. J. Tasaki at Government Institution at Nagoya for the magnetic measurements using the vibrating sample magnetometer. Thanks are also to Drs. K. Kimura and T. Bando at the Institute for Molecular Science for the magnetic measurements at low temperatures.

REFERENCES

1. Anderson, J. R., "Structure of Metallic Catalysts," Academic Press, New York, 1975; Boudart, M., *in* "Advances in Catalysis," Vol. 20, p. 153. Academic Press, New York, 1960; Ueno, A., *Hyomen* (*Surface*) **22,** 18 (1984) [in Japanese].
2. van Hardeveld and Hartog, F., *Surf. Sci.* **15,** 189 (1969); van Hardeveld and van Montfoort, *Surf. Sci.* **4,** 396 (1964).
3. Nakamura, M., Yamada, M., and Amano, A., *J. Catal.* **39,** 125 (1975); Brunelle, J. P., Sugier, A., and Le Page, J. F., *J. Catal.* **43,** 273 (1976).

4. Iwasawa, Y., and Ogasawara, S., *J. Chem. Soc. Faraday Trans. I* **75,** 1465 (1979).
5. Misono, M., Nozawa, Y., and Yoneda, Y., *in* "Proceedings, 6th Int. Congr. Catal.," Vol. 1, p. 386. Chem. Soc., London, 1977; Misono, M., Sakata, K., Ueda, F., Nozawa, Y., and Yoneda, Y., *Bull. Chem. Soc. Japan.* **53,** 648 (1980).
6. Lunde, C. R. F., and Dumesic, J. A., *J. Phys. Chem.* **85,** 3175 (1981), **86,** 130 (1982).
7. Yang, B. L., Fong, F., and Kung, H. H., *J. Phys. Chem.* **88,** 2525 (1984).
8. Yang, B. L., Fong, F., and Kung, H. H., *J. Phys. Chem.* **88,** 2531 (1984).
9. Ueno, A., Suzuki, H., and Kotera, Y., *J. Chem. Soc. Faraday Trans. I* **79,** 127 (1983); Takasaki, S., Suzuki, H., Takahashi, K., Tanabe, S., Ueno, A., and Kotera, Y., *J. Chem. Soc. Faraday Trans. I* **80,** 803 (1984).
10. Tohji, K., Udagawa, Y., Tanabe, S., and Ueno, A., *J. Amer. Chem. Soc.* **106,** 612, 5172 (1984).
11. Cullity, B. D., "X-ray Diffraction." Addison–Wesley, Reading, MA, 1956.
12. Tohji, K., Udagawa, Y., Kawasaki, T., and Masuda, K., *Rev. Sci. Instrument.* **54,** 1482 (1983); Tohji, K., and Udagawa, Y., *Japan J. Appl. Phys.* **22,** 882 (1983).
13. Kimura, K., and Bando, T., *Kotai-Butsuri (Solid State Phys.)* **19,** 467 (1984) [in Japanese].
14. Sato, K., Iwai, M., Sano, H., and Konno, M., *Bull. Chem. Soc. Japan.* **57,** 634 (1984).
15. Via, G. H., Sinfelt, J. H., and Lytle, F. W., *J. Chem. Phys.* **71,** 690 (1979); Lytle, F. W., Wei, P. S. P., Greegor, R. B., Via, G. H., and Sinfelt, J. H., *J. Phys. Chem.* **70,** 4849 (1979); Tohji, K., Udagawa, Y., Tanabe, S., and Ueno, A., *J. Amer. Chem. Soc.* **106,** 612 (1984).
16. Wells, A. F., "Structural Inorganic Chemistry." Oxford Univ. Press, London/New York, 1975.
17. Greegor, R. B., and Lytle, F. W., *J. Catal.* **63,** 476 (1980).
18. Tohji, K., Udagawa, Y., Tanabe, S., and Ueno, A., *J. Amer. Chem. Soc.* **106,** 5172 (1984).
19. Tamaru, K. (ed.). "Hyomen-Kagaku" (Surface Chemistry). Gakkai Pub., 1985 [in Japanese].
20. Okamoto, S., Kobayashi, K., Yasufuku, K., and Sekizawa, H., *Nihon Kagaku Kaishi,* **856** (1984) [in Japanese].
21. Morup, S., and Topsoe, H., *Appl. Phys.* **11,** 63 (1976); Kundig, W., Bommel, H., Constabaris, G., and Lindquist, R. H., *Phys. Rev.* **142,** 327 (1966).
22. Morup, S., Dumesic, J. A., and Topsoe, H., "Application of Mössbauer Spectroscopy" (R. L. Cohen, Ed.). Academic Press, New York, 1980.
23. Okamoto, S., *in* "Proceedings, International Meeting on Highly Dispersed Iron Oxide Cluster and Corrosion" (T. Ekdahl, Ed.). Leningrad, 1981.
24. Andrianov, K. A., "Polymer Reviews," Vol. 6, Interscience, London, 1965; Zeitler, V. A., and Brown, C. A., *J. Phys. Chem.* **51,** 1174 (1957); Nogami, M., and Moriya, Y., *Yogyo-Kyokaishi* **85,** 59 (1977).